Kinetics of Magnetoelastic Twin-Boundary Motion in Ferromagnetic Shape-Memory Alloys

A. Pramanick,[1,2,*] X.-L. Wang,[1,†] A. D. Stoica,[2] C. Yu,[3,4] Y. Ren,[4] S. Tang,[5,6] and Z. Gai[6]

[1]*Department of Physics and Materials Science, City University of Hong Kong, Hong Kong SAR, People's Republic of China*
[2]*Chemical and Engineering Materials Division, Oak Ridge National Laboratory, Oak Ridge, Tennessee 37831, USA*
[3]*State Key Laboratory of Heavy Oil Processing, China University of Petroleum, Beijing 102249, People's Republic of China*
[4]*Advanced Photon Source, Argonne National Laboratory, Argonne, Illinois 60439, USA*
[5]*Department of Materials Science and Engineering, University of Tennessee, Knoxville, Tennessee 37996, USA*
[6]*Center for Nanophase Materials Sciences, Oak Ridge National Laboratory, Oak Ridge, Tennessee 37831, USA*

(Received 22 July 2013; revised manuscript received 12 October 2013; published 30 May 2014)

We report the kinetics of twin-boundary motion in the ferromagnetic shape-memory alloy of Ni-Mn-Ga as measured by *in situ* high energy synchrotron diffraction. The temporal evolution of twin reorientation during the application of a magnetic field is described by thermally activated creep motion of twin boundaries over a distribution of energy barriers. The dynamical creep exponent μ was found to be ~0.5, suggesting that the distribution of energy barriers is a result of short-range disorders.

DOI: 10.1103/PhysRevLett.112.217205 PACS numbers: 75.80.+q, 61.05.C-, 81.40.Lm

Twinning is a primary deformation mode in crystalline solids in which a fraction of the original (parent) lattice is reoriented into its mirror image through a displacement of the lattice points by some integral fraction of spacing between equivalent lattice sites [1]. This is observed for a variety of physical phenomena such as domain switching in ferroelectric or ferroelastic crystals [2,3], transformational plasticity in metals [4,5], and geological seismic wave propagation in Earth's lower mantle [6]. Consequently, understanding the microscopic mechanisms for twinning is of fundamental importance for crystal plasticity. From a technical point of view, twinning plays a central role in the shape-memory behavior of materials used in actuators and biomedical devices [7]. For example, in the martensitic phase of Cu-Al-Ni—a traditional shape-memory alloy—"pseudoelastic" deformation under the application of a mechanical stress occurs by a shear displacement of atoms across twin boundaries; the shearing of the atomic positions causes twin boundaries to propagate through the crystal lattice and thereby constitutes a reversible mode of deformation [8]. Similar pseudoelastic deformation can also be achieved under magnetic actuation as was recently demonstrated in ferromagnetic shape-memory alloys (FSMAs) such as Ni-Mn-Ga [9]. In this latter case, an energy difference is generated between the two martensitic twin variants under a magnetic field, which is proportional to the magnetocrystalline anisotropy energy K_u of the crystal lattice. This energy difference creates an internal shear stress acting on the magnetoelastic interface between the two martensitic twin variants, which in turn induces twin reorientation [10]. The consequent magnetic-field-induced macroscopic strains are particularly attractive for novel functionalities in smart devices [11], and also for energy harvesting [12]. An investigation of the key parameters responsible for the kinetics of twin reorientation is essential to understand the underlying physical mechanisms and to achieve deterministic control for end applications.

Microscopically, twin reorientation proceeds through the process of nucleation and growth [4]. Subsequent to their rapid nucleation, twins of alternate variants grow as a result of sideways motion of twin boundaries, as illustrated in Fig. 1. For twin boundaries, it is energetically more favorable to move sequentially through a transverse propagation of "ledges" or steps (Fig. 1) [13], which constitute interfacial line defects called disconnections.

Usually, the step involving twin-boundary motion is slower than the nucleation of new twin variants, and therefore the overall kinetics of twin reorientation is controlled by twin-boundary motion. During their sideways motion, twin boundaries need to overcome barriers placed by a spatially varying energy landscape consisting of contributions from interatomic potentials and local

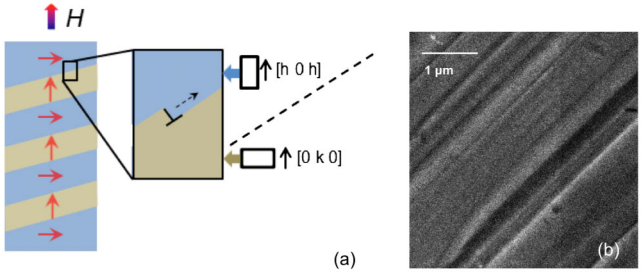

FIG. 1 (color online). (a) Magnetic-field-induced sideways motion of magnetoelastic twin boundaries through transverse propagation of steps associated with twinning disconnections. The crystallographic orientation of the two twin variants are shown in parentheses, and the red arrows indicate magnetic moment directions. (b) Representative microstructure obtained using a scanning electron microscope showing parallel stripes of neighboring twins.

discontinuities [14]. In this respect, twin-boundary motion is analogous to the motion of interfaces in other disordered systems such as 180° ferroelectric [15] or ferromagnetic domain walls [16], solitons in incommensurate crystalline phases [17], and fluid-fluid interfaces in porous systems [18]. However, unlike in these materials, the kinetics of twin-boundary propagation in ferroelastic and martensitic materials in the slow creep regime is far less understood at the moment due to a lack of adequate experimental data [14]. Here, we have examined the kinetics of ferroelastic-ferromagnetic twin-boundary propagation in the martensitic phase of a Ni-Mn-Ga FSMA, which could offer a unique opportunity in this regard.

The generalized laws for interface propagation in disordered media were developed out of the original theory proposed by Avrami to calculate the transformed volume of a growing secondary phase from multiple nuclei within a parent matrix, while taking into account the overlapping regions between different entities [19]. This theory turned into the Kolmorov-Avrami-Ishibashi (KAI) model, which describes the switching kinetics of ferroelectric domains [19]. In this model, the fraction $Q(t)$ of switched volume is given by

$$Q(t) = 1 - \exp(-A), \tag{1}$$

where $\exp(-A)$ is the so called "extended volume" given by $\exp[-(t/t_0)^n]$, t_0 is a characteristic switching time, and n is the effective dimension. The domain-wall velocity v is related to t_0 through the relation $t_0 \sim (1/v)^{n-(1/n)}$ for a continuous generation of nuclei, and $t_0 \sim 1/v$ for instantaneous generation of nuclei [19,20]. The latter applies to the present study, which is growth controlled. In the regime of low-to-moderate driving forces, which is of interest for most practical purposes, v is characteristic of thermally activated "creep" motion of an interface over energy barriers. Since v is dependent on the nature of the pinning potentials, the interaction between a moving interface and pinning sites can be revealed by measuring the switching kinetics between the different crystallographic variants [21].

We used *in situ* high-energy x-ray diffraction to study the kinetics of martensitic twin reorientation in single crystals of Ni-Mn-Ga under the application of magnetic fields. The highly penetrating nature of high-energy x rays, 115 keV, ensures that structural changes representative of the bulk could be directly measured from large internal material volume, and therefore the derived twinning kinetics behavior is not biased by possible artifacts from surface effects [22] or local stress concentrations [23]. The kinetics of twin reorientation measured in Ni-Mn-Ga reveal a distribution of energy barriers for the propagation of magnetoelastic twin boundaries, indicating that twin reorientation in ferromagnetic martensites is far more complicated than being essentially described by a characteristic critical shear stress [10]. Analysis of our data further indicates that the pinning potentials for twin-boundary motion in FSMAs likely have short range forces, a view which could be reconciled with the elastic fields surrounding twinning disconnections [24].

Samples of dimensions $2 \times 2 \times 5$ mm (sample 1) and $1 \times 1 \times 5$ mm (sample 2) were cut from larger single crystals of Ni-Mn-Ga that were obtained from Goodfellow Corporation. In the martensitic state, the alloy has a 5M modulated structure with lattice parameters $a = 4.255$ Å, $b = 5.613$ Å, and $c = 4.216$ Å. The martensitic transformation temperatures are $T_M = (M_s + M_f)/2 = 48\,^{\circ}\mathrm{C}$ [25]. The lattice spacings for the two reflections of interest are $d_{040} = 1.4$ Å and $d_{202} = 1.5$ Å, following the simplified martensitic notation [26]. Further details on sample composition and microstructure are provided in the Supplemental Material [27]. Additional details on the crystallographic structure and magnetic properties of alloys of similar composition can be found elsewhere [25].

The microstructure of both single crystal samples consists of fine martensitic twins in the form of parallel stripes with a typical width of about 1 μm; see the representative micrograph in Fig. 1(b), which is typical of self-accommodated twinning arrangements [24]. A few variant boundaries were also observed, which separated regions with different orientations of the parallel twin stripes.

The *in situ* x-ray diffraction experiments were carried out at the beam line 11-ID-C of the Advanced Photon Source, Argonne National Laboratory. Further details on diffraction geometry are provided in the Supplemental Material [27]. Application of a magnetic field causes one of the twin variants (such as represented in blue or dark gray in Fig. 1) to reorient by ~90° so as to align the magnetic easy axis [0 k 0] parallel to the field direction. This is accompanied by correlated intensity changes of 040 and 202 diffraction peaks, which can be observed during the application of a magnetic field, as shown in Figs. 2(a) and 2(b) [26]. Magnetic fields in increments of 0.1 T were applied using a superconducting magnet with the field direction perpendicular to the x-ray beam direction. For each increment, the field magnitude was kept constant for 1800 sec [Fig. 2(c)], during which diffraction patterns of ~20 sec each were recorded as a function of time. Integrated intensities over five scans were averaged to reduce the scatter of the kinetics data, possibly due to individual stochastic events, leading to an effective time resolution of 100 sec. At each instant, the volume fraction R of the twins with their [0 k 0] axis parallel to the magnetic field is calculated using

$$R = \frac{I_{040}}{I_{040} + kI_{202}}, \tag{2}$$

where I is the integrated intensity of a particular diffraction peak denoted by the specific subscript, and $k = (F_{040}/F_{202})^2$ in which F are the structure factors of the respective reflections. Here, $k \sim 1$.

Figure 2(d) shows the values of R measured for sample 1, at the beginning and end of each field value. R increases with increasing magnetic field as more twins are reoriented

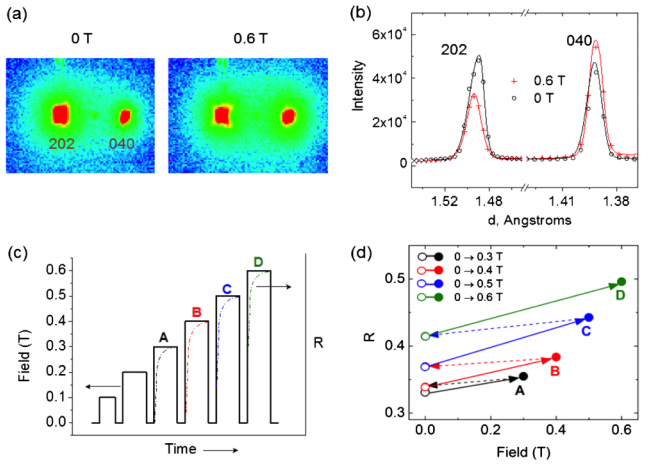

FIG. 2 (color online). Magnetic-field-induced twin reorientation observed from change in relative intensities of 040 and 202 Bragg diffraction peaks. (a) Diffraction spots on image plate detector (a), and peak profiles (b), for 040 and 202 reflections. (c) Measurement plan for *in situ* diffraction patterns. (d) Change in volume fraction of twin variants R with increasing field as calculated from Eq. (2).

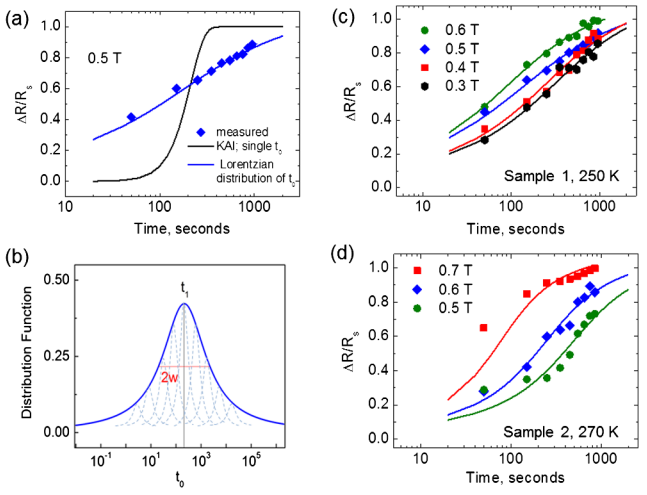

FIG. 3 (color online). (a) The measured temporal response of twin reorientation (solid diamonds) is compared with the predictions from two different models. The plot shows that the kinetics of twin reorientation cannot be described with a single switching time t_0. A finite distribution, such as the one shown (b), needs to be considered. The twin reorientation kinetics for sample 1 at 250 K and for sample 2 at 270 K are shown in (c) and (d), respectively.

with their magnetic easy axis [0 k 0] parallel to the applied field. Within the time period when the field is kept constant, a temporal increase in R is followed by an eventual saturation at longer times, as schematically illustrated in Fig. 2(c). For a constant field magnitude, twin reorientation can be exhausted as the twin boundaries become stuck in some local minima. Such behavior was observed earlier for martensitic twin boundaries in Cu-Ni-Al under the application of constant stress fields [8]. With subsequent increase in field magnitude, a larger volume of twins is reoriented as higher input driving forces cause further twin-boundary motion. Also, as can be seen from Fig. 2(d), a minor fraction of the reoriented twins revert back to their original state, possibly due to the presence of a small fraction of a special type of twin microstructure as identified by Straka *et al.* in Ref. [28].

Figure 3(a) shows the relative change in volume fraction of twins $\Delta R/\Delta R_s$ as a function of time for sample 1 under an applied magnetic field H of 0.5 T at 250 K. Here, ΔR and ΔR_s are the instantaneous and the saturated values of change in R, respectively, for a particular applied field. The solid black line in Fig. 3(a) is the expected kinetic behavior for a twin orientation mechanism with a single time constant t_0 of 160 sec, as described in Eq. (1). Figure 3(a) clarifies that the twin reorientation process cannot be described with a single time constant, but instead it consists of events with a distribution of characteristic switching times $\langle t_0 \rangle$. Therefore, we modified Eq. (1) as follows:

$$\frac{\Delta R}{R_s} = \int_{-\infty}^{\infty} \{1 - \exp[-(t/t_0)^n]\} F(\log t_0) d(\log t_0), \qquad (3)$$

where, $F(\log t_0)$ describes a plausible distribution of characteristic switching times t_0 [21]. A satisfactory fit to the measured data was obtained for a Lorentzian distribution function for $F(\log t_0)$,

$$F(\log t_0) = \frac{A}{\pi}\left[\frac{w}{(\log t_0 - \log t_c)^2 + w^2}\right], \qquad (4)$$

where t_c is a central value and $2w$ is the full width at half maximum of the distribution, and A is a normalization constant [Fig. 3(b)] [29]. The numerical integration for Eq. (3) was implemented in IGOR Pro.

Note that t_0 is dependent on the height of the energy barrier that an interface has to overcome for crossing over from one state to the other through thermal fluctuations. Therefore, in essence, t_0 represents an energy scale. A finite distribution of t_0 implies that the energy barrier (or critical force) for twin reorientation is characterized by a distribution function rather than a single value. Therefore, the observed kinetics of twin reorientation can neither be satisfactorily described by an average velocity as reported in Ref. [30], nor by the overly simplified assumption of a single critical shear stress such as in Ref. [10]. Some indications of broad pinning effects could be deduced from jumplike behaviors in magnetically induced strains [31,32], and individual stochastic avalanche-type events of twin-boundary motion [23]. Here, the direct structural measurements with high-energy x-ray diffraction from bulk millimeter-sized crystals provided explicit evidence, and a quantitative description, for broad energy barriers in the form of a statistical distribution of the switching times t_0.

The kinetics of twin reorientation at two different temperatures, 250 K for sample 1 and 270 K for sample 2, for a

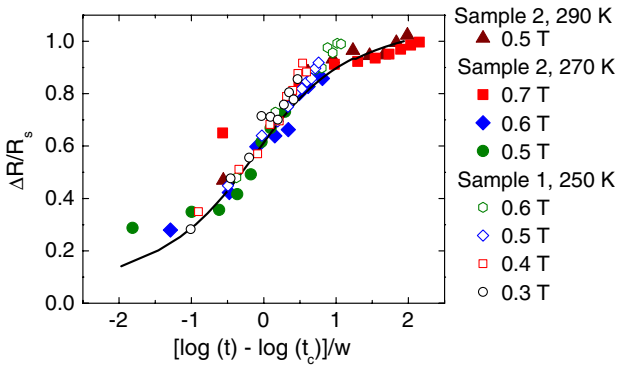

FIG. 4 (color online). Twin reorientation kinetics as a function of normalized time $[\log(t) - \log(t_c)]/w$ for different applied fields and temperatures.

range of magnetic fields, can be successfully described by the statistical laws for interface driven growth, as shown in Figs. 3(c) and 3(d), respectively. As the temperature or applied field increases, the curve moves to the left with faster time scales. Figure 4 shows all $\Delta R/\Delta R_s$ subsequent to their rescaling as a function of $[\log(t) - \log(t_c)]/w$. All data curves, regardless of the temperature or magnetic field collapse on top of each other over three decades of time, which establishes the growth law for twin reorientation kinetics with H applied parallel to [0 k 0] of the reoriented twins. Such unified scaling behavior was observed earlier for domain-wall switching in ferroelectric materials and had been attributed to thermally activated creep motion of domain walls [21].

We now discuss the types of energy barriers that could be responsible for the observed twin reorientation kinetics. In recent studies of the dynamic response of FSMAs under a pulsed magnetic field, Faran and Shilo identified a bimodal distribution of energy barriers: a Peierls energy barrier, which is the activation energy for twin wall motion in a defect free crystal lattice, and a twinning stress, which is the required driving force in the presence of imperfections or defects [33,34]. It was shown that twinning kinetics is predominantly dictated by twinning stresses when the frequency of the applied field falls below 1 Hz [35]; the present study, carried out under a long duration of constant magnetic fields, therefore falls within this regime. Within the twinning stresses, there are two types: the type I stress is strongly temperature dependent and increases rapidly below the martensitic transition temperature, whereas the type II stress is small (~0.1 MPa) and only weakly temperature dependent [36]. The data in Figs. 3(c)–3(d) reveals that the distribution of t_0 or the energy barrier for twinning is both field and temperature dependent. Furthermore, measurements made at room temperature (290 K) for applied fields of 0.5, 0.6, and 0.7 T showed that while the same scaling relationship as derived above applies for the data for 0.5 T (see Fig. 4), it fails to satisfactorily describe the observed behavior at fields higher than 0.5 T for this temperature. This follows from the precipitous decrease in type I twinning stresses with temperature, which makes the type I twinning stress comparable to the usually much smaller type II twinning stress as the martensitic transition temperature ($T_M \sim 321$ K) is approached [36]. As a consequence, when a higher driving force is imparted by increasing the magnetic field, the mobilities of previously pinned type I and type II twin boundaries become comparable and the kinetics of the type I and type II boundaries can no longer be distinguished from the experimental data at 290 K. Therefore, the overall strong temperature dependence of energy barriers for twinning as revealed by the experimental data suggests that the type I twinning stress should be the primarily force responsible for the observed twinning kinetics.

In an attempt to gain further physical insights into possible interactions underpinning the observed twin-boundary motion kinetics, we examined the numerical fitting results with a creep model. A thermally activated creep is generally observed due to the glassy characteristic of randomly pinned interfaces in a disordered medium. The defects, which locally modify the energy barrier for interface migration, create a spatially varying pinning potential. The overall creep of an interface arises as a competition between elastic forces that tend to keep the surfaces flat and the effect of defects, which promotes local wandering of the interface [37,38]. Assuming that the energy landscape is characterized by a unique energy scale, and that the energy differences between neighboring metastable states are the same as the energy barriers separating them, one obtains the velocity v of a propagating interface as $v \propto \exp[-\beta U_c(f_c/f)^{\mu}]$, where $\beta = 1/kT$, U_c is a scaling energy constant, f_c is a critical force for interface propagation at $T = 0$ K, and μ is a characteristic exponent that reflects the correlation length of the disorder [16]. If the disorder is characterized by long-range fields, then μ is closer to 1, while for shorter range fields μ is lower. As a first approximation, we use $v \sim 1/t_c$ for growth-controlled kinetics and consider the driving force for twin-boundary motion to be linearly proportional to the applied field magnitude H. We can then use the expression $\log(t_{c(1)})/\log(t_{c(2)}) \propto (H_2/H_1)^{\mu}$ to estimate the value of μ. Fitting with Eq. (3) shows that for sample 1 at 250 K, $t_{c(1)} \sim 295$ sec for $H_1 = 0.4$ T and $t_{c(2)} \sim 105$ sec for $H_2 = 0.6$ T, which gives $\mu \sim 0.5$. A similar analysis for sample 2 at 270 K, for applied fields of 0.5 T and 0.6 T, provides $\mu \sim 0.6$. The observed value here of $\mu \sim 0.5$–0.6 for magnetoelastic twin boundaries is consistent with what could be expected for a 2D interface pinned by defects having short-range elastic forces [16]. It is considerably different than $\mu \sim 1$ observed for domain wall motion leading to ferroelectric switching in $Pb(Zr_{0.2}Ti_{0.8})O_3$ epitaxial films, which the authors of Ref. [15] attributed to long-range internal fields of ionic defects. Quite possibly, the short-range elastic forces in FSMAs (for $\mu \sim 0.5$) come from twinning disconnections

and complex dislocation structures, as alluded to in previous studies [13,24,39]. Here, we must emphasize, however, that the above viewpoint for twin-boundary creep involving elastic defects is one plausible mechanism that is consistent with the observed experimental data. Further studies, both experimental and theoretical, are necessary in order to unambiguously determine the complex magnetoelastic interactions that occur during progressive twin-boundary motion.

In summary, direct *in situ* measurements of twinning kinetics in a FSMA using high-energy x-ray diffraction revealed that thermally activated magnetoelastic twin-boundary motion occurs over a distribution of energy barriers under low-to-moderate driving forces. Numerical fitting of the kinetics data is consistent with a creep model involving short-range local disorders, a likely origin for which is twinning disconnections.

This research was sponsored by the Laboratory Directed Research and Development Program of Oak Ridge National Laboratory (ORNL), managed by UT-Battelle, LLC for the U. S. Department of Energy under Contract No. DE-AC05-00OR22725. X.-L. W. acknowledges the support by a grant from the Research Grants Council of Hong Kong Special Administrative Region (Project No. CityU 122713). Use of the Advanced Photon Source (APS), an Office of Science User Facility operated for the U.S. Department of Energy (DOE) Office of Science by Argonne National Laboratory, was supported by the U.S. DOE under Contract No. DE-AC02-06CH11357. Technical assistance from Richard Spence during experiments at APS is gratefully acknowledged. A portion of this research was conducted at the Center for Nanophase Materials Sciences, which is sponsored at Oak Ridge National Laboratory by the Scientific User Facilities Division, Office of Basic Energy Sciences, U.S. Department of Energy.

*Corresponding author.
apramani@cityu.edu.hk
†Corresponding author.
xlwang@cityu.edu.hk

[1] G. Dieter, *Mechanical Metallurgy* (McGraw-Hill, Boston, MA, 1986), 3rd ed..
[2] G. Tutuncu, D. Damjanovic, J. Chen, and J. L. Jones, Phys. Rev. Lett. **108**, 177601 (2012).
[3] E. K. H. Salje, Phase Transit. **83**, 657 (2010).
[4] J. W. Christian and S. Mahajan, Prog. Mater. Sci. **39**, 1 (1995).
[5] G. Puglisi and L. Truskinovsky, Continuum Mech. Thermodyn. **14**, 437 (2002).
[6] E. K. H. Salje, A. Buckley, G. Van Tendeloo, Y. Ishibashi, and G. L. Nord, Jr., Am. Mineral. **83**, 811 (1998).
[7] S. A. Wilson *et al.*, Mater. Sci. Engg. R **56**, 1 (2007).
[8] R. Abeyaratne, C. Hu, and R. D. James, Philos. Mag. A **73**, 457 (1996).
[9] K. Ullakko, J. K. Huang, C. Kantner, R. C. O'Handley, Appl. Phys. Lett. **69**, 1966 (1996).
[10] R. C. O'Handley, S. J. Murray, M. Marioni, H. Nembach, and S. M. Allen, J. Appl. Phys. **87**, 4712 (2000).
[11] O. Söderberg, I. Aaltio, Y. Ge, O. Heczko, and S. P. Hannula, Mater. Sci. Eng. A **481**, 80 (2008).
[12] P. Müllner, V. A. Cherenko, and G. Kostorz, Scr. Mater. **49**, 129 (2003).
[13] R. Abeyaratne and S. Vedantam, J. Mech. Phys. Solids **51**, 1675 (2003).
[14] X. Ding, T. Lookman, Z. Zhao, A. Saxena, J. Sun, and E. K. H. Salje, Phys. Rev. B **87**, 094109 (2013).
[15] T. Tybell, P. Paruch, T. Giamarchi, and J.-M. Triscone, Phys. Rev. Lett. **89**, 097601 (2002).
[16] S. Lemerle, J. Ferré, C. Chappert, V. Mathet, T. Giamarchi and P. Le Doussal, Phys. Rev. Lett. **80**, 849 (1998).
[17] C. Reichhardt, C. J. Olson, and F. Nori, Phys. Rev. B **58**, 6534 (1998).
[18] N. Martys, M. Cieplak, and M. O. Robbins, Phys. Rev. Lett. **66**, 1058 (1991).
[19] M. Avrami, J. Chem. Phys. **7**, 1103 (1939); **8**, 212 (1940).
[20] Y. Ishibashi and Y. Takagi, J. Phys. Soc. Jpn. **31**, 506 (1971).
[21] J. Y. Jo, H. S. Han, J.-G. Yoon, T. K. Song, S.-H. Kim, and T. W. Noh, Phys. Rev. Lett. **99**, 267602 (2007).
[22] Y. Ge, O. Heczko, O. Söderberg, S.-P. Hannula, Scr. Mater. **54**, 2155 (2006).
[23] R. I. Barabash, C. Kirchlechner, O. Robach, O. Ulrich, J.-S. Micha, and O. M. Barabash, Appl. Phys. Lett. **103**, 021909 (2013).
[24] P. Müllner, V. A. Chernenko, and G. Kostorz, J. Magn. Magn. Mater. **267**, 325 (2003).
[25] A. Pramanick, K. An, A. D. Stoica, and X.-L. Wang, Scr. Mater. **65**, 540 (2011).
[26] A. Pramanick, X. P. Wang, K. An, A. D. Stoica, J. Yi, Z. Gai, C. Hoffmann, and X.-L. Wang, Phys. Rev. B **85**, 144412 (2012).
[27] See Supplemental Material at http://link.aps.org/supplemental/10.1103/PhysRevLett.112.217205 for additional details on sample composition, microstructure and geometry of diffraction experiments.
[28] L. Straka, H. Hänninen, N. Lanska, and A. Sozinov, J. Appl. Phys. **109**, 063504 (2011).
[29] A. M. Stoneham, Rev. Mod. Phys. **41**, 82 (1969).
[30] Y.-W. Lai, R. Schäfer, L. Schultz, and J. McCord, Acta Mater. **56**, 5130 (2008).
[31] N. I. Glavatska, A. A. Rudenko and V. A. L'vov, J. Magn. Magn. Mater. **241**, 287 (2002).
[32] N. Glavatska, Mater. Sci. Engg. A **481–482**, 73 (2008).
[33] E. Faran and D. Shilo, J. Mech. Phys. Solids **59**, 975 (2011).
[34] E. Faran and D. Shilo, J. Mech. Phys. Solids **61**, 726 (2013).
[35] E. Faran and D. Shilo, Appl. Phys. Lett. **100**, 151901 (2012).
[36] O. Heczko, V. Kopecký, A. Sozinov, and L. Straka, Appl. Phys. Lett. **103**, 072405 (2013).
[37] T. Nattermann, Y. Shapir, and I. Vilfan, Phys. Rev. B **42**, 8577 (1990).
[38] P. Chauve, T. Giamarchi and P. Le Doussal, Phys. Rev. B **62**, 6241 (2000).
[39] P. Müllner, Z. Clark, L. Kenoyer, W. B. Knowlton, and G. Kostorz, Mater. Sci. Engg. A **481–482**, 66 (2008).